ISSN 1070-3632, Russian Journal of General Chemistry, 2006, Vol. 76, No. 7, pp. 1031–1040. © Pleiades Publishing, Inc., 2006.
Original Russian Text © L.I. Savostina, R.M. Aminova, V.F. Mironov, 2006, published in Zhurnal Obshchei Khimii, 2006, Vol. 76, No. 7, pp. 1078–1087.

To the Problem of the Reaction Mechanism of 2-Methoxybenzo[*d*]-1,3,2-dioxaphosphorin-4-one with Chloral on the Basis of Quantum-Chemical Calculations: II.[1] The Perkov Reaction

L. I. Savostina[a], R. M. Aminova[a], and V. F. Mironov[b]

[a] *Kazan State University, Kazan, Tatarstan, Russia*
[b] *Arbuzov Institute of Organic and Physical Chemistry, Kazan Scientific Center, Russian Academy of Sciences ul. Arbuzova 8, Kazan, Tatarstan, 420088 Russia*

Received September 27, 2005

Abstract — The Perkov reaction mechanism on an example of 2-methoxybenzo[*d*]-1,3,2-dioxaphosphorin-4-one reaction with chloral was investigated by means of quantumchemical calculations [PM3, DFT (PBE functional, "Triple z" basis, "Priroda" program)]. The primary reaction step is shown to include [1+2]-cycloaddition to form an intermediate with pentacoordinated phosphorus atom (oxaphosphirane-containing spirophosphorane) which transforms further to vinyl phosphate. Structure of the transition state on the pathway to vinyl phosphate is close to dichlorovinyloxyquasiphosphonium cation with the chloride counterion. Thermodynamic parameters of the starting compounds and reaction products as well as activation energies of the processes are evaluated.

DOI: 10.1134/S107036320607005X

Phosphorylated cyclic derivatives of salycilic acid, 2-alkoxybenzo[*d*]-1,3,2-dioxaphosphorin-4-ones, readily react with activated carbonyl compounds to form seven-membered heterocycles, benzo[*f*]-1,3,2-dioxa- and benzo[*f*]-1,4,2-dioxaphosphepines [1-7]. Reaction of 2-alkoxybenzo[*d*]-1,3,2-dioxaphosphorin-4-ones with halocarbonyl compounds such as chloral and bromal may proceed in two directions: by the pathway leading to benzo[*f*]-1,4,2-dioxaphosphepines (at 20°C) and by the Perkov reaction pathway (at 150°C) [8]. The authors [8,9] have previously thoroughly studied the first reaction pathway by the methods of quantum chemistry on an example of 2-methoxybenzo[*d*]-1,3,2-dioxaphosphorin4-one **I** reaction with chloral leading to 2-methoxy-2-trichloromethylbenzo[*f*]-1,4,2-dioxaphosphepin-5-one. Considering great significance of the Perkov reaction leading to practically important vinyl phosphates exhibiting biological activity [10], in the present work we carried out theoretical investigation of this reaction mechanism on an example of phosphite **I** reaction with chloral. Note that the Perkov reaction mechanism is sufficiently complicated and its quantum chemistry study has never been reported.

The Perkov reaction of compound **I** with chloral gives two phosphates, **II** and **III** [8]. The acyclic derivative **II** under the same reaction conditions undergoes cyclization to 2-(1,1-dichlorovinyloxy)benzo-[*d*]-1,3,2-dioxyphosphorin-2,4-dione **III**.

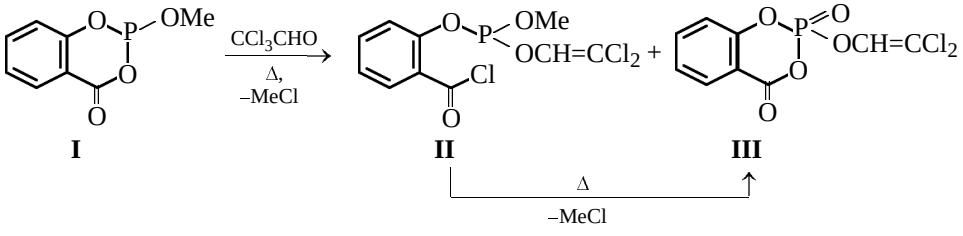

[1] For communication I, see [1].

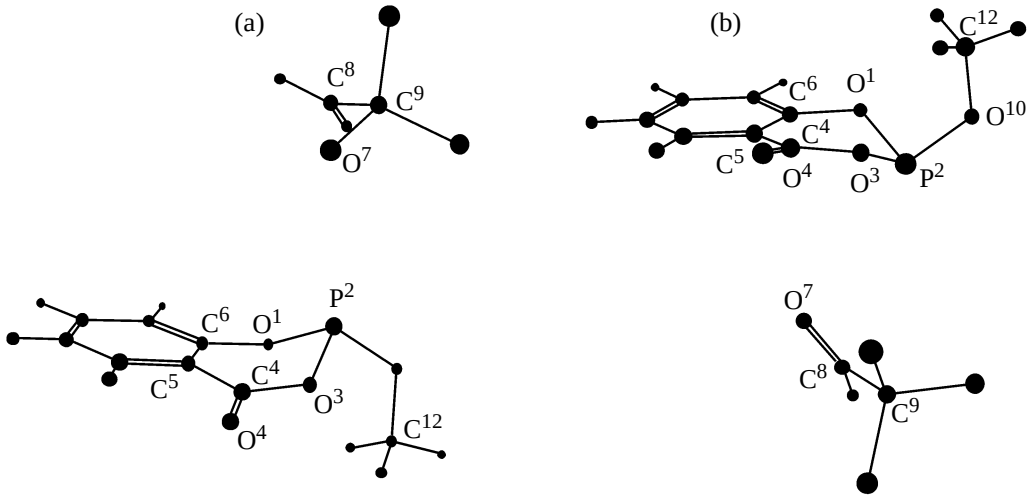

Fig. 1. Steric arrangement of prereaction complexes (a) and (b).

In the present work the formation of acyclic vinylphosphate **II** was studied by PM3 and DFT (using PBE functional and "Triple z" basis [12]) methods of quantum chemistry. Calculation of stationary points was carried out with complete optimization of all geometric parameters. Vibrational spectra were calculated for all the stationary points. Besides, calculation of internal reaction coordinate was carried out for all the found transition states.

Results of the quantum chemistry calculations of the Perkov reaction mechanism leading to formation of vinylphosphate **II** show that the first reaction step is [1+2]-cycloaddition (cheletropic reaction) of phosphite **I** to chloral molecule resulting in formation of intermediate spirophosphorane **IV** with pentacoordinate phosphorus atom. Parameters of the starting compounds (phoshite **I** and chloral) and intermediate **IV** for some configurations and conformations have been established by us previously [1].

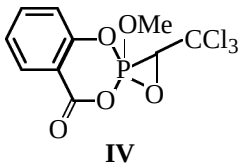

IV

Depending on the direction of the phosphorus atom attack on the carbonyl carbon atom of chloral molecule (phosphorus atom acts as nucleophile, and the carbonyl carbon atom of chloral as electrophile [13]) the calculation leads to two different structures of the prereaction complex: **a** and **b**. These structures with the energies –2482.789427 and –2482.79023714 a.u. are shown in Figs. 1a, 1b. Both the prereaction complexes are more stable than the reagents (by 0.6 and 1.17 kcal mol^{-1} respectively, as compared with the sums of energies of the reagents). In the prereaction complex **a** the $P^2\cdots O^7$ and $P^2\cdots C^8$ distances are 4.0 and 4.3 Å, and in the complex **b** –3.7 and 4.2 Å respectively. In the course of calculations sixteen spirophosphorane intermediates containing threemembered $P^2O^7C^8$ heterocycle **1**–**16** were obtained. Such a variety of the possible intermediates is caused by configurational and conformational isomerism and is connected with the different location of OMe, CCl_3, and H substituents (in threemembered ring), orientation of oxaphosphirane ring respectively to the endocyclic carbonyl group (the oxygen atom in the $P^2O^7C^8$ fragment located *cis* or *trans* to this group), and also by the different configuration of phosphorus and C^8 atoms. Some steric structures of the calculated intermediates and their energies are shown in Figs. 2 and 3.

Detailed analysis of the steric arrangement of intermediates **1**–**16** shows that for the formation of acyclic vinylphosphate **II** the structures **2** and **10** (Figs. 2 and 3) are the most favorable. As is seen, orientation of one chlorine atoms in CCl_2 group of the intermediates is favorable for the subsequent attack on the endocyclic carbonyl group of the six-membered heterocycle.

In the intermediate **10** the six-membered heterocycle has the *sofa* conformation with small deflection of P^2 atom from the plane of the six-membered ring. Threemembered $P^2O^7C^8$ ring occupies axial position relatively to the six-membered heterocycle and is turned in the direction providing location of O^7 oxygen atom in *anti* position to the $C^4{=}O^4$ carbonyl group. Methoxy group occupies equatorial position. Phosphorus atom has trigonal bipyramide configuration distorted to the square pyramide form. The oxygen O^7 atom of oxaphosphirane heterocycle and

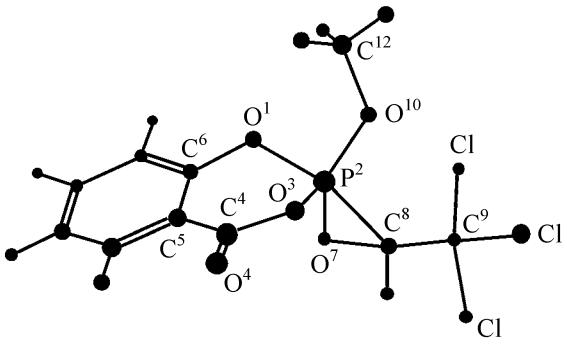

1 (−2482.77760144)

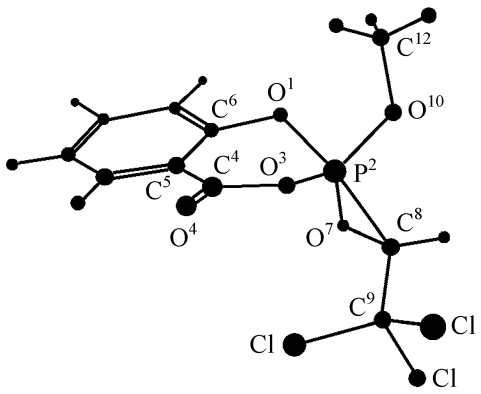

2 (−2482.77667319)

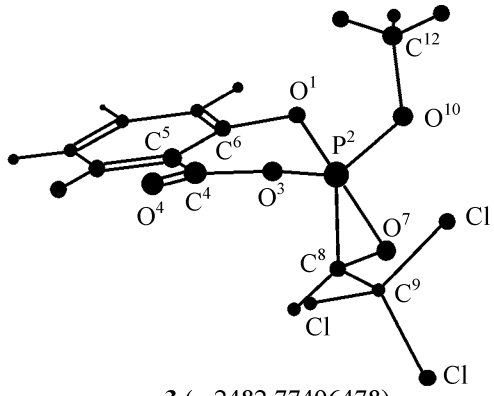

3 (−2482.77496478)

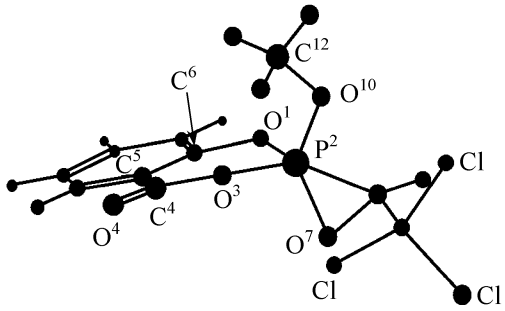

4 (−2482.77668457)

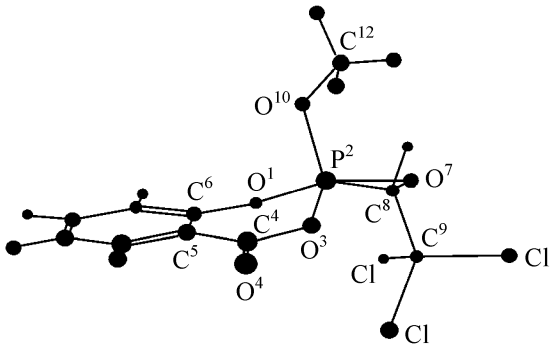

5 (−2482.77975409)

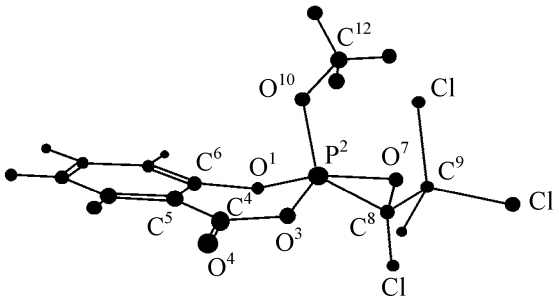

6 (−2482.77992705)

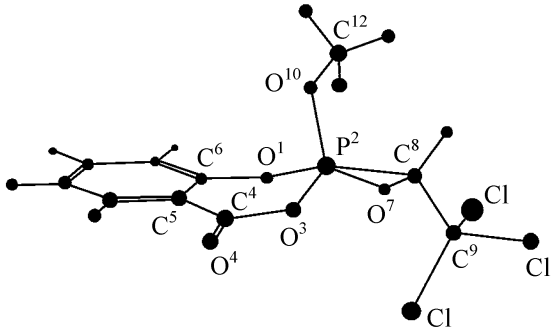

7 (−2482.77801168)

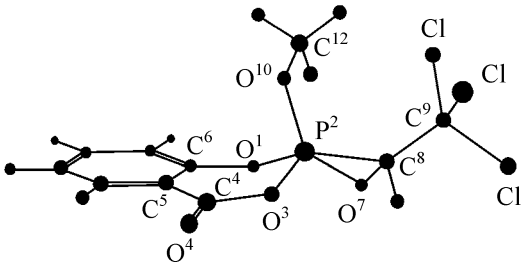

8 (−2482.778041)

Fig. 2. Structure of intermediates **1**–**8** containing oxaphosphirane heteroring (total molecule energy in a.u. is given in brackets).

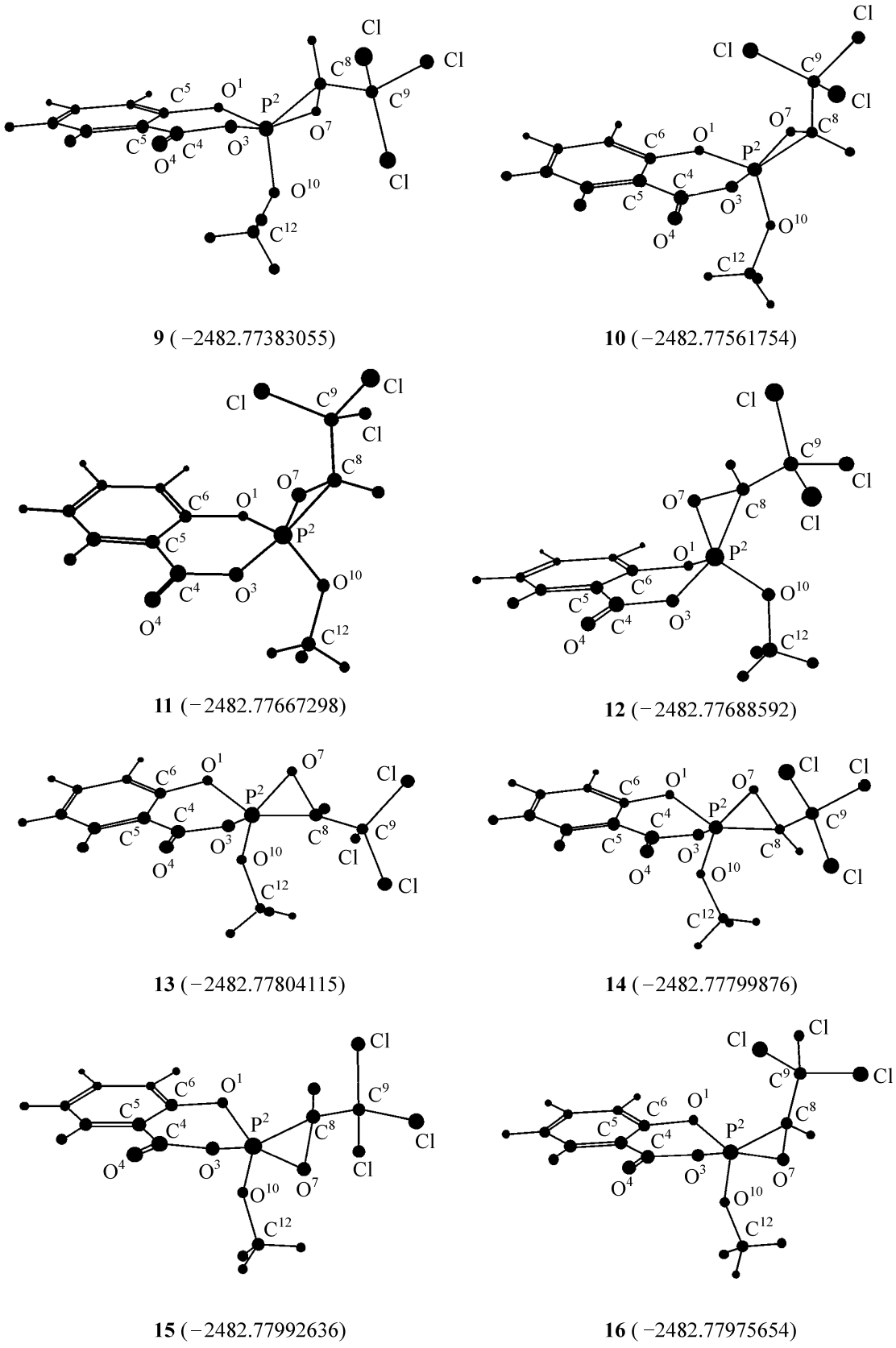

Fig. 3. Structure of intermediates **9**–**12** containing oxaphosphirane heteroring (total molecule energy in a.u. is given in brackets).

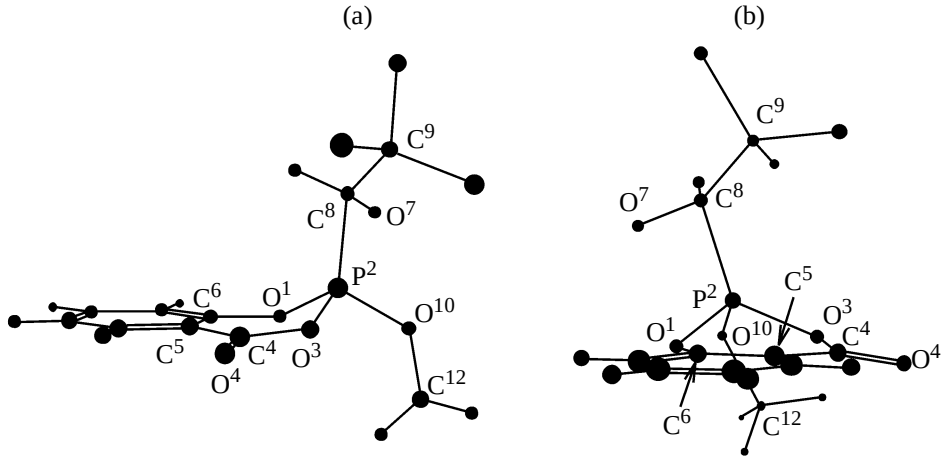

Fig. 4. Steric structure of the transition state TS_1: (a) view from the side of carbonyl group and (b) view from the side of phenyl fragment.

the substituent $O^3C^4{=}O^4$ are located in axial positions of the trigonal bipyramide. The bipyramide distortion degree may be judged about from the valye of $O^3P^2O^7$ bond angle (156.3°). The C^9Cl_3 group at C^8 atom and P^2–O^1 bond are *cis*-located relatively to the plane of the threemembered heterocycle.

In the intermediate **2** the phosphorus atom configuration (trigonal bipyramide) is also strongly distorted to the form of square pyramide. In this case O^1 and C^8 atoms are located closer to the axial orientation (147.3°). The sixmembered heterocycle conformation is a distorted *bath*. The P^2 and O^3 atoms are deflected to the some side of its planar fragment ($O^1C^6C^5C^4$) but by different values. Oxaphosphirane ring is located in axial position, and methoxy group is equatorial. Trichloromethyl group and O^3 atom occupy *cis* positions relatively to the plane of the three membered ring.

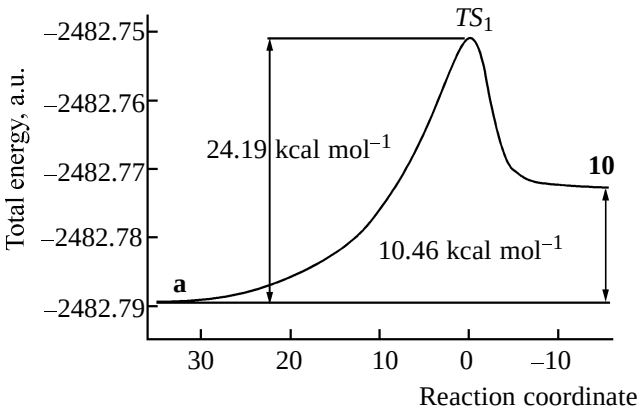

Fig. 5. Plot of the total energy on the reaction coordinate for the transition state TS_1.

On the pathway from prereaction complex to spirophosphorane **10** we obtained transition state TS_1 (its frequency 292.0i, energy 2482.750882 a.u.). Its structure is shown in Fig. 4. Geometric parameters (interatomic distances, bond and torsion angles of prereaction complex **a**, the transition state TS_1, and oxaphosphirane intermediate **10** are listed in the table. It is seen that P^2–C^8 bond (1.84 Å) in the transition state TS_1 is significantly longer than in the intermediate **10** (1.79 Å). At the same time the C^8–O^7 bond length also alters significantly: 1.2 Å in the prereaction complex **a**, 1.32 Å in the transition state TS_1, and 1.48 Å in the intermediate **10**. Calculation of internal reaction coordinate (IRC) shows that the transition state TS_1 found really lies on the pathway from the prereaction complex **a** (Fig. 1a) to spirophosphorane **10**. In Fig. 5 is shown a plot of the total energy of the reaction system on the reaction coordinate. As seen, in this phase the reaction is exothermal. The heat of reaction is 10.46 kcal mol^{-1} and activation energy is 24.19 kcal mol^{-1}.

Further calculations outline the result very important in respect of chemical kinetics. Formation of $C^8{=}C^9$ double bond (Fig. 6) proceeds simultaneously with elimination of the chlorine atom Cl^{13} from the C^9Cl_3 group and the P^2–C^8 bond cleavage of oxaphosphirane cycle. In the course of this process the sp^3-hybridized C^8 atom becomes sp^2-hybridized. In the appearing $C^7{=}C^8(Cl^{14})Cl^{15}$ fragment the $C^7{=}C^8$ bond length is 1.39 Å. This value falls between the single and double bond lengths. Chlorine C^{13} atom is shifted out from the C^9 carbon atom to 2.35 Å. The structure formed is regarded as a transition state TS_2. It is characterized by imaginary frequency 353.1*i* and the energy –2482.730549 a.u. Phosphorus atom in the

Selected values of bond lengths and interatomic distances (Å), bond and torsion angles (deg) of prereaction complexes **a** and **b**, transition states TS_1, TS_2, TS_3, and TS_4, intermediates **10** and **2**, and acyclic vinylphosphate **II**, calculation by DFT method using the "Priroda" program [11]

Parameter	**a**	TS_1	**10**	TS_2	**b**	TS_3	**2**	TS_4	**II**
Interatomic distance or bond length									
P^2–O^1	1.71	1.64	1.65	1.62	1.71	1.64	1.71	1.63	1.65
P^2–O^3	1.71	1.69	1.71	1.58	1.71	1.62	1.65	1.59	1.49
$P^2\cdots O^7$ (P^2–O^7)	4.01	2.19	1.68	1.58	3.70	2.15	1.64	1.57	1.64
P^2–C^8 ($P^2\cdots C^8$)	4.34	1.84	1.79	2.26	4.21	1.81	1.81	2.32	2.62
O^7–C^8	1.20	1.32	1.48	1.48	1.20	1.35	1.52	1.48	1.39
C^8–C^9	1.55	1.57	1.51	1.39	1.55	1.56	1.51	1.38	1.34
O^3–C^4 ($O^3\cdots C^4$)	1.39	1.40	1.38	1.50	1.39	1.44	1.42	1.49	3.18
O^4–C^4	1.21	1.21	1.21	1.19	1.21	1.20	1.20	1.19	1.20
C^9–Cl^{13} ($C^9\cdots Cl^{13}$)	1.80	1.81	1.80	2.35	1.76	1.79	1.79	2.31	6.63
$C^4\cdots Cl^{13}$ (C^4–Cl^{13})	5.09	4.19	4.16	2.88	4.35	4.11	3.48	2.98	1.84
Bond angle									
$O^1P^2O^3$	97.1	100.5	98.8	107.7	97.6	104.9	97.5	104.6	114.6
$O^1P^2O^7$	95.9	89.4	99.1	117.6	99.3	90.2	95.5	104.1	103.7
$O^1P^2C^8$	102.9	105.9	110.8	93.2	111.2	108.6	147.3	141.2	109.9
$O^1P^2O^{10}$	99.7	107.6	108.8	103.7	99.4	101.8	95.2	105.7	100.5
$P^2O^3C^4$	122.4	124.0	124.8	124.1	124.2	119.7	126.8	122.8	91.7
$P^2C^8O^7$	66.4	86.1	60.7	44.1	57.6	84.6	58.2	42.1	33.3
$P^2C^8C^9$	90.3	117.9	125.9	126.3	93.6	119.7	132.6	128.9	122.5
$P^2O^7C^8$	97.7	56.9	68.8	95.0	106.5	56.9	69.7	98.7	119.1
$O^7C^8C^9$	124.4	120.8	116.6	119.1	124.3	119.7	115.0	114.7	122.1
$O^3P^2O^{10}$	100.0	101.2	94.7	107.5	100.2	103.9	110.9	108.7	121.4
$O^3P^2C^8$	128.3	128.7	108.2	101.1	95.0	115.8	104.8	94.3	89.8
$O^3C^4O^4$	119.2	118.7	119.6	115.7	118.9	117.2	117.4	116.1	84.5
$C^6O^1P^2$	115.8	117.9	120.7	117.9	117.7	118.4	119.3	115.4	119.5
$O^7P^2C^8$	15.9	37.1	50.5	40.9	15.9	38.5	52.1	38.2	27.6
$O^3P^2O^7$	144.2	165.4	156.3	118.6	86.4	89.8	123.5	124.7	116.0
$O^{10}P^2O^7$	110.5	85.8	94.1	99.9	159.1	158.5	122.3	107.6	97.7
$O^{10}P^2C^8$	122.2	111.1	129.9	140.0	143.5	120.0	98.8	99.7	121.1
$C^8C^9Cl^{13}$	105.9	108.6	106.9	111.9	112.9	112.7	114.9	111.2	49.7
Torsion angle									
$C^9C^8P^2O^{10}$	–82.3	–72.9	–47.7	–110.4	42.9	57.1	139.5	169.3	–65.1
$O^3P^2C^8C^9$	57.2	52.2	65.1	24.9	–71.7	–68.9	24.9	59.5	62.3
$O^1P^2O^3C^4$	–45.8	–39.8	–41.1	–19.5	41.2	44.4	34.5	34.5	18.6
$O^1P^2O^7C^8$	117.5	118.1	109.5	59.6	140.1	120.5	174.6	–164.5	107.0
$O^1P^2C^8O^7$	–64.9	–66.6	–84.6	–130.0	–42.8	–65.4	–10.0	24.4	–81.3
$O^1P^2O^{10}C^{12}$	–51.5	–81.2	–78.3	–64.5	52.0	57.8	20.9	73.8	–76.1
$P^2O^3C^4O^4$	–163.5	–164.6	–159.8	166.3	165.5	155.6	170.9	–177.5	62.2
$P^2O^3C^4C^5$	18.3	17.1	23.4	–3.9	–16.4	–30.6	–9.4	–4.8	–67.1
$P^2O^7C^8C^9$	72.9	120.3	118.1	113.5	69.8	121.2	126.1	121.5	101.6
$O^3P^2O^{10}C^{12}$	47.5	23.8	22.6	49.4	–47.5	–51.1	–79.1	–38.1	51.4
$O^4C^4C^5C^6$	–166.1	–170.7	–173.5	–152.6	167.2	178.3	166.1	153.9	–25.6
$C^5C^6O^1P^2$	–34.6	–29.5	–22.9	–28.6	32.5	18.4	34.3	33.1	–80.7
$C^6O^1P^2O^3$	52.2	44.0	38.8	35.3	–47.6	37.3	–45.9	–47.8	39.3
$C^6O^1P^2O^{10}$	153.7	149.5	136.9	149.0	–149.3	–145.4	–157.9	–162.4	171.2
$C^6O^1P^2O^7$	–94.3	–125.1	–125.6	–101.9	39.9	52.6	78.9	84.4	–88.1
$C^6O^1P^2C^8$	–79.8	–91.6	–74.5	–67.4	50.8	87.0	86.8	68.8	–60.0

Table (Contd.)

Parameter	**a**	TS_1	**10**	TS_2	**b**	TS_3	**2**	TS_4	**II**
				Torsion angle					
$P^2C^8C^9Cl^{13}$	–61.9	–68.9	–103.1	–50.3	54.2	48.3	19.1	–27.4	–49.2
$P^2C^8C^9Cl^{14}$	–178.3	173.4	138.8	–158.2	–67.6	–73.9	–103.1	81.6	–145.1
$P^2C^8C^9Cl^{15}$	60.2	53.3	17.7	62.0	176.2	168.2	139.9	–141.3	35.1
$O^7C^8C^9Cl^{13}$	–123.1	–171.9	–174.9	–102.6	1.7	–53.2	–49.8	–74.7	–88.8
$O^7C^8C^9Cl^{14}$	120.6	70.4	67.0	149.5	–120.1	–175.4	–171.9	34.3	175.3
$O^7C^8C^9Cl^{15}$	–0.9	–49.7	–54.0	9.7	123.7	66.7	71.1	171.4	–4.5

transition state TS_2 has distorted tetrahedral configuration. Structure of the transition state TS_2 is shown in Fig. 6, its geometric parameters are listed in the table. Elimination of chlorine atom and formation of double bond are accompanied by certain elongation of C^4–O^3 bond, to 1.49 Å as compared with the value of the C^4–O^3 bond length 1.39 Å in the intermediate **10**. This can be explained by the effect of chlorine atom Cl^{13} which in the transition state TS_2 approaches C^4 atom of the C^4–O^3 fragment at a distance of 2.88 Å. Starting with the structure of the transition state TS_2 we carried out calculation of internal reaction coordinate. Lowering in one direction lead to the intermediate **10**, and in another direction to the reaction product, the acyclic vinyl phosphate **II**. Selected geometric parameters of the intermediate **10** and vinyl phosphate **II** are listed in the table. Fig. 7 shows a plot of the total energy dependence on the reaction coordinate. Note that the processes on this reaction pathway are exothermal. The activation barrier is 26.39 kcal mol^{-1}, and the reaction energy in this fragment is 24.65 kcal mol^{-1}.

Taking the structure **2** as the starting intermediate we obtained transition states TS_3 (which is characterized by the imaginary frequency 236.1*i* and energy –2482.75938155 a.u.) and TS_4 (its frequency is 389.8*i* and energy –2482.72615987 a.u.). The transition states TS_1/TS_3 and TD_2/TS_4 differ in the configurations of both phosphorus and carbon atoms. In the transition states TS_1/TS_2 the fragment of chloral molecule is located above the sixmembered heterocycle (view from the side of benzo substituent with the location of C^4O^4 on the right) while in the transition states TS_3/TS_4 it is located below the sixmembered heterocycle. The structure of TS_3 is shown in Fig. 8, and its geometric parameters are listed in the table. Considering the total energy dependence on the reaction coordinate shown in Fig. 9 we calculated activation and reaction barriers (19.37 and 8.38 kcal mol^{-1} respectively). In the transition state TS_4 the Cl^{13} atom is located at a distance 2.31 Å from C^9 atom and at 2.98 Å from C^4 atom. The C^4–O^3 bond of sixmembered heterocycle weakens and elongates to 1.49 Å as compared to the length of this bond

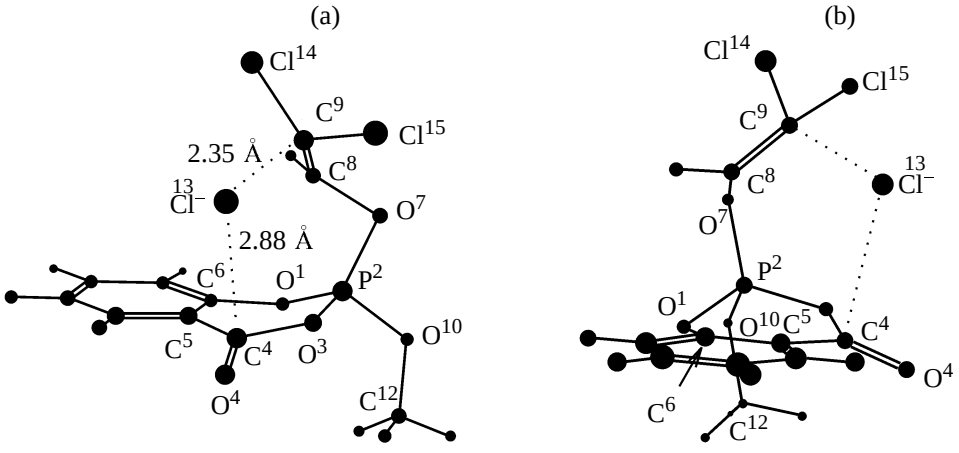

Fig. 6. Steric arrangement of transition state TS_2: (a) view from the side of carbonyl group and (b) view from the side of phenyl fragment.

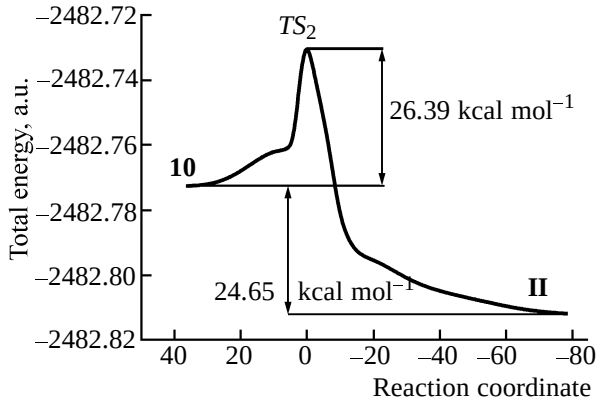

Fig. 7. Plot of the total energy dependence on the reaction coordinate for the transition state TD_2.

(1.42 Å) in the intermediate **2**. The structure of TS_4 is shown in Fig. 10, and its geometric parameters are listed in the table. The internal reaction coordinate calculations for the transition states TS_3 and TS_4 show that lowering from the peak in one direction leads either to the prereaction complex **b** or to the intermediate **2**, while in another direction to the intermediate **2** or to acyclic vinyl phosphate **II**. Geometric parameters of the two latter structures are given in the table. In the Fig. 11 the total energy dependence on the reaction coordinate is plotted. The activation barrier of this reaction is 31.69 kcal mol^{-1}, and the energy of the reaction in this fragment is 21.55 kcal mol^{-1}.

Basing on the results of calculations of the formation mechanism of vinyl phosphate **II** we considered in details the pathway of the bimolecular Perkov reaction. Comparing our calculations with the published data we have to note that reactions of phosphorus-containing compounds with unsaturated reagents have been considered previously [10, 13, 14]. Theoretical consideration of reaction of the model phosphites with carbonyl compounds showed [13] that it proceeds through the formation of threemembered cyclic intermediate (POC). Our calculations show that in the first step of the Perkov reaction the cyclic intermediate **IV** of spirophosphorane structure having oxaphosphirane

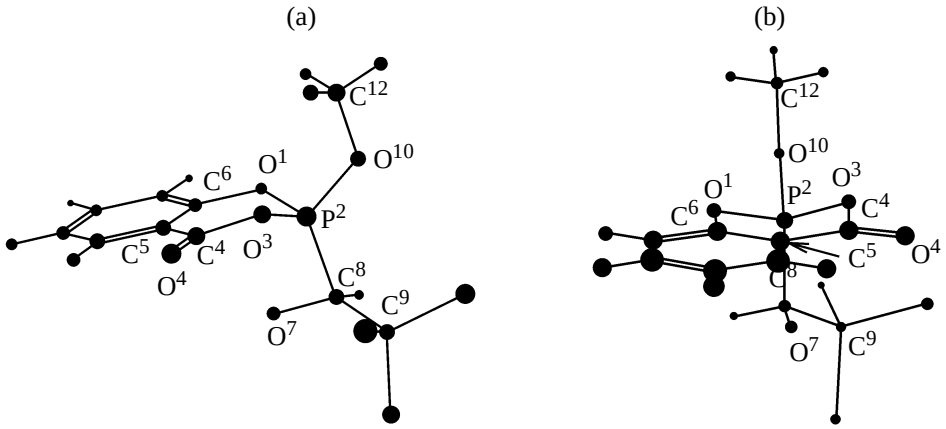

Fig. 8. Steric arrangement of transition state TS_3: (a) view from the carbonyl group and (b) view from the phenyl fragment.

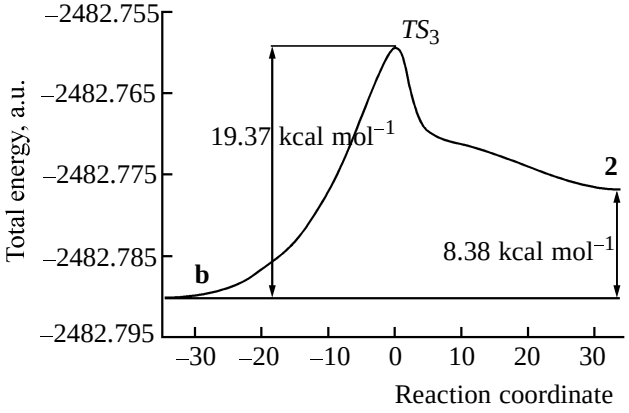

Fig. 9. The total energy dependence on the reaction coordinate for the transition state TS_3.

cycle is also formed. Subsequent reaction has been postulated to proceed [10, 14] through the formation of structures **V**–**VII** resembling quasiphosphonium salts though no strict quantum chemical calculations have been carried out.

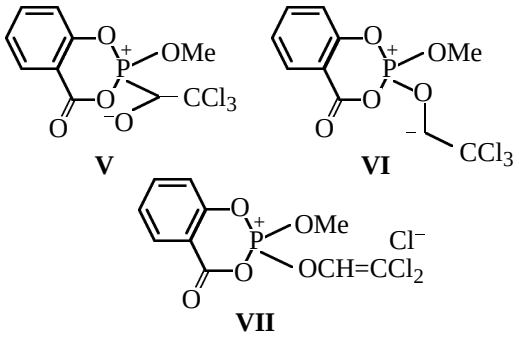

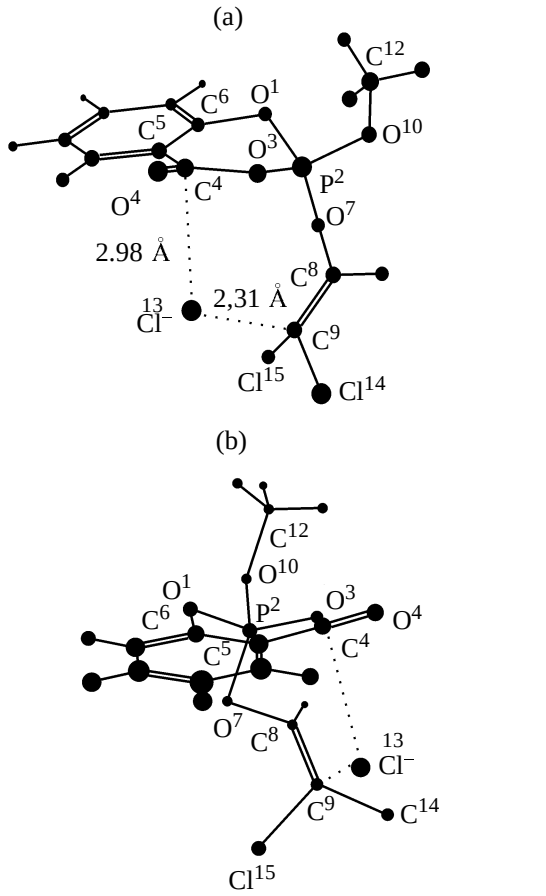

Fig. 10. Steric arranegement of the transition state TS_4: (a) view from the carbonyl group, (b) view from the phehyl fragment.

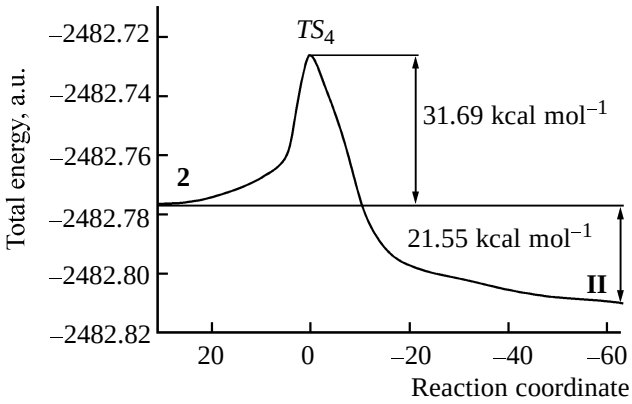

Fig. 11. The total energy dependence on the reaction coordinate for the transition state TS_4.

Our calculations showed that the structure **VI** can not be found on this reaction pathway as an intermediate or as a transition state. Transformation of spiriphosphorane **IV** to vinyl phosphate **II** proceeds with almost simultaneous formation of $C^8{=}C^9$, $P^2{=}O^3$, and $C^4(O^4){-}Cl^{13}$ bonds due to the concerted cleavage of $P^2{-}C^8$, $C^4(O^4){-}^3$, and $C^9{-}Cl^{13}$ bonds. Parameters of TS_1 and TS_3 transition states on this pathway (depending on the direction of the chloral attack on the salicyl phosphite molecule) are close to that of the proposed in literature intermediate **VII**.

Note the common nature of intermediate **IV** on the Perkov reaction pathway and that leading to seven-membered heterocycle [12].

Consideration of quantimchemical calculations of CH_3 group elimination with chlorine atom and cyclic phosphate **III** formation in the course of the Perkov reaction will be presented in subsequent piblications.

ACKNOWLEDGMENTS

The authors express their deep gratitude to D.N. Laikov and Yu.A. Ustynyuk for submitting the "Priroda" program.

The work was carried out with the financial support of NIS-6213.2006.2 grant.

REFERENCES

1. Aminova, R.M., Shamov, G.A., Savostina, L.I., and Mironov, V.F., *Zh. Obshch. Khim.*, 2006, in press.
2. Mironov, V.F., Konovalova, I.V., Mavleev, P.A., Mukhtarov, A.Sh., Ofitserov, E.N., and Pudovik, A.N., *Zh. Obshch. Khim.*, 1991, vol. 61, no. 10, p. 2150.
3. Mironov, V.F., Burnaeva, L.M., Konovalova, I.V., Khlopushina, G.A., Mavleev, R.A., Chernov, P.P., and Pudovik, A.N., *Zh. Obshch. Khim.*, 1993, vol. 63, no. 1, p. 25.
4. Mironov, V.F., Burnaeva, L.A., Krokhalev, V.M., Saloutin, V.I., Konovalova, I.V., Mavleev, R.A., and Chernov, P.P., *Zh. Obshch. Khim.*, 1992, vol. 62, no. 6, p. 1425.
5. Mironov, V.F., Mavleev, R.A., Burnaeva, L.A., Konovalova, I.V., Pudovik, A.N., and Chernov, P.P., *Izv. Akad. Nauk, Ser. Khim.*, 1993, no. 3, p. 565.
6. Mironov, V.F., Konovalova, I.V., Burnaeva, L.M., Khlopushina, G.A., and Shastina, Yu.S., *Zh. Obshch. Khim.*, 1994, vol. 64, no. 7, p. 1217.
7. Mironov, V.F., Burnaeva, L.M., Khlopushina, G.A., Konovalova, I.V., Kurykin, M.A., and Rakhmatullin, A.I., *Izv. Akad. Nauk, Ser. Khim.*, 1996, no. 12, p. 3008.
8. Mironov, V.F., Burnaeva, L.M., Gubaidullin, A.T., Litvinov, I.A., Konovalova, I.V., Zyablikova, T.A.,

Ivkova, G.A., and Romanov, S.V., *Zh. Obshch. Khim.*, 1998, vol. 68, no. 3, p. 399.

9. Mironov, V.F., Litvinov, I.A., Gubaidullin, A.T., Aminova, R.M., Burnaeva, L.M., Azancheev, N.M., Filatov, M.E., and Konovalova, I.V., *Zh. Obshch. Khim.*, 1998, vol. 68, no. 7, p. 1080.
10. Aminova, R.M., Mironov, V.F., and Filatov, M.E., *Zh. Obshch. Khim.*, 1999, vol. 69, no. 1, p. 58.
11. Luknitski, F., *Chem. Rev.*, 1975, vol. 75, no. 3, p. 259.
12. Laikov, D.N., *Chem. Phys. Lett.*, 1997, vol. 281, p. 151.
13. Chang, J.-W.A., Taira, K., Uranov, S., and Gorenstein, D.G., *Tetrahedron*, 1987, vol. 43, no. 17, p. 3863.
14. Vladimirova, I.L., Grapov, A.F., and Lomakona, V.I., *Reaktsii i metody issledovaniya organicheskikh soedinenii* (Reactions and Methods of Investigation of Organic Compounds), Moscow: Khimiya, 1966, vol. 16.